High-power diode-end-pumped laser with multi-segmented Nd-doped yttrium vanadate

Y. J. Huang and Y. F. Chen*

Department of Electrophysics, National Chiao Tung University, Hsinchu, Taiwan
*yfchen@cc.nctu.edu.tw

Abstract: A $Nd:YVO_4$ crystal consisting of three segments with different doping concentrations is originally developed for power scaling in diode-end-pumped solid-state laser. We systematically make a comparison of laser characteristics between the multi-segmented and conventional composite crystals to show the feasibility of using gain medium with multiple doping concentrations for power scale-up in end-pumped laser without introducing significant thermally accompanied effects. We further construct a dual-end-pumped actively Q-switched oscillator at 1064 nm to verify the usefulness of our crystal design, where the largest pulse energy of 1.06 mJ and the highest output power of 45 W are efficiently generated.

OCIS codes: (140.3380) Laser materials; (140.3480) Lasers, diode-pumped; (140.3540) Lasers, Q-switched; (140.3530) Lasers, neodymium; (140.3580) Lasers, solid-state; (140.6810) Thermal effects.

References and links

1. F. Hanson, "Improved laser performance at 946 and 473 nm from a composite $Nd:Y_3Al_5O_{12}$ rod," Appl. Phys. Lett. **66**(26), 3549–3551 (1995).
2. M. Tsunekane, N. Taguchi, T. Kasamatsu, and H. Inaba, "Analytical and experimental studies on the characteristics of composite solid-state laser rods in diode-end-pumped geometry," IEEE J. Sel. Top. Quantum Electron. **3**(1), 9–18 (1997).
3. Z. Zhuo, T. Li, X. Li, and H. Yang, "Investigation of $Nd:YVO_4/YVO_4$ composite crystal and its laser performance pumped by a fiber coupled diode laser," Opt. Commun. **274**(1), 176–181 (2007).
4. X. Li, X. Yu, F. Chen, R. Yan, M. Luo, J. Yu, and D. Chen, "Power scaling of directly dual-end-pumped $Nd:GdVO_4$ laser using grown-together composite crystal," Opt. Express **18**(7), 7407–7414 (2010).
5. Y. J. Huang, Y. P. Huang, H. C. Liang, K. W. Su, Y. F. Chen, and K. F. Huang, "Comparative study between conventional and diffusion-bonded Nd-doped vanadate crystals in the passively mode-locked operation," Opt. Express **18**(9), 9518–9524 (2010).
6. D. Kracht, R. Wilhelm, M. Frede, K. Dupré, and L. Ackermann, "407 W end-pumped multi-segmented Nd:YAG laser," Opt. Express **13**(25), 10140–10144 (2005).
7. R. Wilhelm, D. Freiburg, M. Frede, and D. Kracht, "End-pumped Nd:YAG laser with a longitudinal hyperbolic dopant concentration profile," Opt. Express **16**(24), 20106–20116 (2008).
8. R. Wilhelm, M. Frede, and D. Kracht, "Power scaling of end-pumped solid-state rod lasers by longitudinal dopant concentration gradients," IEEE J. Quantum Electron. **44**(3), 232–244 (2008).
9. Y. F. Chen, "Design criteria for concentration optimization in scaling diode end-pumped lasers to high powers: influence of thermal fracture," IEEE J. Quantum Electron. **35**(2), 234–239 (1999).
10. X. Yan, Q. Liu, X. Fu, Y. Wang, L. Huang, D. Wang, and M. Gong, "A 108 W, 500 kHz Q-switching $Nd:YVO_4$ laser with the MOPA configuration," Opt. Express **16**(5), 3356–3361 (2008).
11. Z. Xiang, D. Wang, S. Pan, Y. Dong, Z. Zhao, T. Li, J. Ge, C. Liu, and J. Chen, "Beam quality improvement by gain guiding effect in end-pumped $Nd:YVO_4$ laser amplifiers," Opt. Express **19**(21), 21060–21073 (2011).
12. Q. Liu, H. Chen, X. Yan, and M. Gong, "36.5 W high beam quality 532 nm green laser based on dual-rod AO Q-switched resonator," Opt. Commun. **284**(13), 3383–3386 (2011).
13. Y. J. Huang, P. Y. Chiang, H. C. Liang, K. W. Su, and Y. F. Chen, "Efficient high-power UV laser generated by an optimized flat-flat actively Q-switched laser with extra-cavity harmonic generations," Opt. Commun. **285**(1), 59–63 (2012).
14. Q. Liu, X. Yan, M. Gong, H. Liu, G. Zhang, and N. Ye, "High-power 266 nm ultraviolet generation in yttrium aluminum borate," Opt. Lett. **36**(14), 2653–2655 (2011).

1. Introduction

The main limiting factors for power scaling in end-pumped solid-state laser are remarkable thermal gradient and accompanied mechanical tensile stress inside the gain medium, which come from the fact that the homogeneous doping within the active element leads to the exponential decay of the pump light along the longitudinal direction. The composite crystal, where the pump facet of an uniformly doped material is bonded with an undoped matrix to serve as a heat sink, has recently proven its usefulness in reducing the spatial gradient of the temperature and alleviating the thermally induced mechanical stress [1–5]. More recently, it was shown that the Nd:YAG crystal composed of multiple segments with increasing doping concentrations in the pump direction can further flatten the longitudinal temperature and stress distributions to permit a higher pump power before the thermal fracture occurs [6–8]. Under the maximum pump power of 750 W, the continuous-wave (CW) output power of 407 W with the optical conversion efficiency of 54% was achieved in an end-pumped multi-segmented Nd:YAG laser [6].

Compared with the Nd:YAG crystal, the Nd:YVO_4 crystal is characterized by its broad absorption bandwidth as well as high absorption coefficient around 808 nm, large stimulated emission cross section, and natural birefringence. These features make the Nd:YVO_4 crystal highly desirable for developing a high-power, high-repetition-rate Q-switched laser with linearly polarized emission. However, so far the concept of the multiple segments with different doping concentrations has not been realized in the Nd:YVO_4 crystal to our knowledge. In this work, we originally design a multi-segmented Nd:YVO_4 crystal consisting of three parts with successive doping concentrations of 0% (undoped crystal), 0.1%, and 0.3%. A compact linear cavity is subsequently constructed to make a thorough comparison between the multi-segmented and conventional composite crystals, including the laser performance in the CW operation, the sensibility to the diode temperature, and the thermal-lensing effect. We further apply this novel active element to develop a high-power dual-end-pumped actively Q-switched laser at 1064 nm. Under an absorbed pump power of 110 W, this pulsed laser is able to efficiently generate the largest pulse energy of 1.06 mJ at 40 kHz and the highest output power of 45 W at 100 kHz. Experimental results manifestly disclose that employing the multi-segmented crystal enables the attainable pump power in the end-pumped laser comparable to the level in the side-pumped system, while keeping the high optical conversion efficiency and excellent beam quality due to a good overlapping between the spatial distributions of the pump and laser modes.

2. Experimental setup

The experimental arrangement for exploring the laser performance of the multi-segmented and conventional composite crystals is schematically depicted in Fig. 1(a). We prepared three types of the Nd:YVO_4 materials (Witcore) as sketched in Figs. 1(b)-1(d). The first one was a conventional composite YVO_4/Nd:YVO_4 crystal with a 2-mm-long undoped YVO_4 crystal bonded to a 0.1-% doping Nd:YVO_4 crystal with the length of 16 mm (YVO_4/0.1% Nd:YVO_4). The second one was another conventional composite YVO_4/Nd:YVO_4 crystal with a 2-mm-long undoped YVO_4 crystal bonded to a 0.2-% doping Nd:YVO_4 crystal with the length of 12 mm (YVO_4/0.2% Nd:YVO_4). The last one was a multi-segmented YVO_4/Nd:YVO_4 crystal with a 2-mm-long undoped YVO_4 crystal bonded to a 0.1-% doping Nd:YVO_4 crystal with the length of 8 mm, and followed by a 0.3-% doping Nd:YVO_4 crystal with the length of 5 mm (YVO_4/0.1% + 0.3% Nd:YVO_4). The crystallographic *c* axes of the bonded materials for all laser crystals were better than 0.2 degree. All laser crystals were cut along the *a* axes and with the cross sections of 3 mm × 3 mm, and both surfaces of the gain media were coated to be anti-reflective at 808 and 1064 nm. The relationship between the absorption coefficient α at 808 nm and the Nd doping concentration N_d is given by $\alpha = 2 \cdot N_d$ mm^{-1} [9]. Therefore, the pump absorptions for the YVO_4/0.1% Nd:YVO_4, YVO_4/0.2% Nd:YVO_4, and YVO_4/0.1% + 0.3% Nd:YVO_4 crystals were estimated to be 95.9%, 99.2%, and 99%, respectively. During the experiment, they were wrapped with indium foil and mounted in water-cooled copper heat sinks at 18þC.

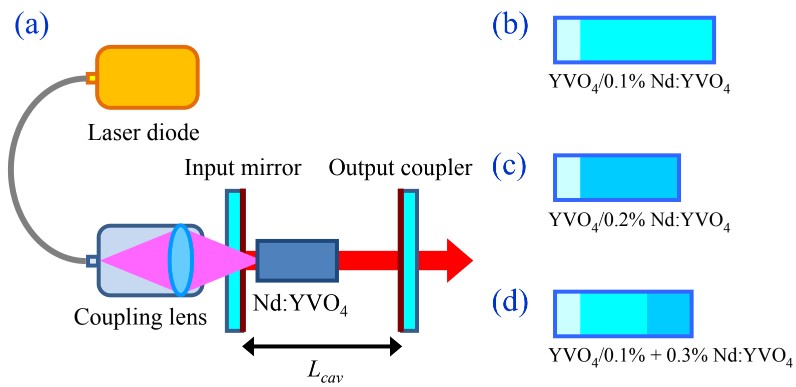

Fig. 1. (a) Experimental arrangement for the comparison of the multi-segmented and conventional composite crystals; Schematic configurations for the (b) YVO_4/0.1% Nd:YVO_4, (c) YVO_4/0.2% Nd:YVO_4, and (d) YVO_4/0.1% + 0.3% Nd:YVO_4 crystals.

The cavity configuration was a plane-parallel cavity. The flat input mirror was coated for high transmission at 808 nm on the pump surface, and it was anti-reflection coated at 808 nm and high reflection coated at 1064 nm on the other surface. A flat mirror with a reflectivity of 80% at 1064 nm was utilized as the output coupler, which was experimentally found to be the optimal reflectivity. The pump source was a fiber-coupled laser diode (Lumics) with a numerical aperture of 0.22 and a core diameter of 600 μm, whose emission wavelength was around 808 nm and could be finely tuned by varying the temperature of the laser diode. A convex lens with a focal length of 25.4 mm and a coupling efficiency of 95% was employed to reimage the pump radiation inside the gain medium with a magnification ratio of unity. The cavity length L_{cav} of approximately 20 mm was set for the construction of an extremely compact CW laser, which was experimentally found to give the best performance in output power for each laser crystals.

3. Comparative study between multi-segmented and conventional composite crystals

The output powers for each crystal were optimized at the maximum absorbed pump powers. The emission wavelength during the experiment was experimentally confirmed to be centered around 1064 nm. Figure 2 shows the dependences of the output power at 1064 nm on the absorbed pump power at 808 nm for each gain media. The pump thresholds for all active elements are found to be almost the same, around 11 W. The maximum output power is 26.9 W for the YVO_4/0.1% Nd:YVO_4 crystal under an absorbed pump power of 55.4 W, corresponding to the optical conversion efficiency of 49.4%. It is experimentally observed that the conventional composite crystal with higher doping concentration can generally accomplish higher optical conversion efficiency. Under an absorbed pump power of 56 W, the maximum output power of 28.5 W with the optical conversion efficiency of 50.9% is achieved for the YVO_4/0.2% Nd:YVO_4 crystal. For the YVO_4/0.1% + 0.3% Nd:YVO_4 crystal, the maximum output power is up to 30.9 W under an absorbed pump power of 56.7 W. The corresponding optical conversion efficiency obtained with this novel multi-segmented crystal is significantly enhanced to be 54.5% as compared with the conventional composite crystals. The beam quality factors for each case were generally better than 1.7. It is worthwhile to mention that the thermal fracture near the interface of the undoped and doped parts for the YVO_4/0.2% Nd:YVO_4 crystal was observed once the absorbed pump power was beyond 56 W, as can be clearly revealed in Fig. 2. Lowering the doping concentration of the doped material is essentially helpful in avoiding a potential risk of the thermal fracture, for example, using the YVO_4/0.1% Nd:YVO_4 crystal. However, the crystal length of the doped segment needs to be increased for sufficient absorption of the pump light, which indicates the mode matching efficiency should be optimized with careful consideration. Comparatively speaking, using a Nd:YVO_4 crystal with multiple doping concentrations is a convenient and practical

#190751 - $15.00 USD Received 17 May 2013; revised 16 Jun 2013; accepted 21 Jun 2013; published 27 Jun 2013

means to simultaneously scale the output power in the end-pumped laser system and diminish the temperature-dependent mechanical stress peak inside the gain medium.

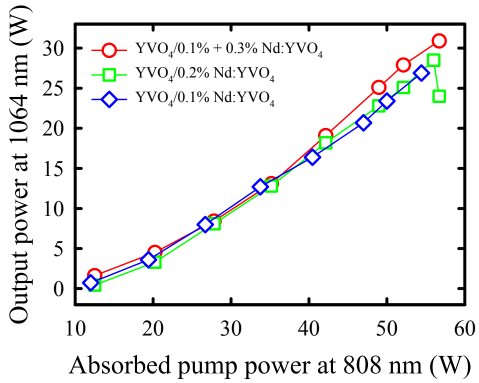

Fig. 2. Output powers with respect to the absorbed pump power for each laser crystal.

We then experimentally built the relationships between the output power and the temperature of the laser diode for all laser crystals, as shown in Fig. 3(a). Note that Fig. 3(a) is equivalent to estimating the sensibility of the laser performance to the emission wavelength of the laser diode. Here we define the full width at the 90% of the maximum output power as the effective bandwidth in temperature. It is experimentally observed that the output performance obtained from the YVO_4/0.2% Nd:YVO_4 and YVO_4/0.1% + 0.3% Nd:YVO_4 crystals have broader temperature tolerances as compared with that obtained from the YVO_4/0.1% Nd:YVO_4 crystal, where the effective bandwidths are evaluated to be around 11.4, 13.5, and 13.6þC for the YVO_4/0.1% Nd:YVO_4, YVO_4/0.2% Nd:YVO_4, and YVO_4/0.1% + 0.3% Nd:YVO_4 crystals, respectively.

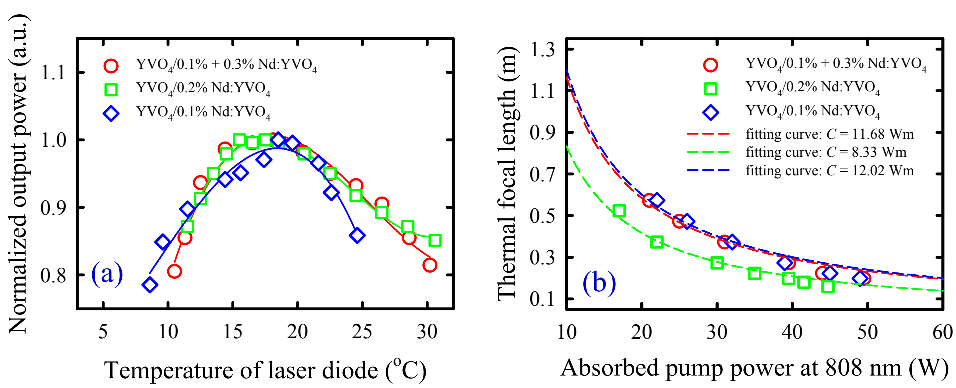

Fig. 3. (a) Normalized output powers versus the temperature of the laser diode, and (b) thermal focal lengths as a function of the absorbed pump power, for each laser crystal.

We also properly adjusted the cavity length to determine the effective focal lengths of the thermal lens via a stability criterion at different absorbed pump powers. As a result, the degree of the thermal-lensing effect can be estimated with the empirical formula of $f_{th} = C / P_{abs}$, where f_{th} denotes the thermal focal length, P_{abs} stands for the absorbed pump power, and C is the proportional constant representing the extent of the thermal-lensing effect. Note that the larger magnitude of the proportional constant, the weaker the thermal-lensing effect. Referring to Fig. 3(b), the thermal-lensing effect for the YVO_4/0.2% Nd:YVO_4 crystal is evidently stronger than that for the YVO_4/0.1% Nd:YVO_4 one, in which the proportional constants are determined to be 12.02 and 8.33 Wm for the YVO_4/0.1% Nd:YVO_4 and YVO_4/0.2% Nd:YVO_4 crystals, respectively. Moreover, it is intriguing that the proportional

#190751 - $15.00 USD Received 17 May 2013; revised 16 Jun 2013; accepted 21 Jun 2013; published 27 Jun 2013

constant of 11.68 Wm for the YVO_4/0.1% + 0.3% Nd:YVO_4 crystal is nearly identical to the value for the YVO_4/0.1% Nd:YVO_4 crystal. This observation is resulted from the relatively uniform temperature distribution along the longitudinal direction in the multi-segmented crystal, which effectively weakens the thermal-lensing effect.

4. Application of multi-segmented crystal for actively Q-switched operation

In order to demonstrate the applicability of the multi-segmented crystal, we designed a dual-end-pumped actively Q-switched oscillator based on our YVO_4/0.1% + 0.3% Nd:YVO_4 crystal, as schematically displayed in Fig. 4(a). The pump sources, coupling lenses, and the input mirror were the same as those described in Fig. 1(a). The pump beams were reimaged inside the laser crystals with the spot radii of around 450 μm. The folded mirror had the identical coating characteristics to the input mirror, except that the angle of incidence was intended to be 45þ. The output coupler was a flat mirror with a reflectivity of 55% at 1064 nm. A 20-mm-long acousto-optical (AO) Q-switch (Gooch & Housego) was placed in the center of the cavity to fulfill the pulsed operation in the range from 40 to 100 kHz. The AO Q-switch was AR coated at 1064 nm on both sides, and it was driven at a central frequency of 41 MHz with a RF power of 25 W. The overall length of the laser cavity was set around 220 mm. A fast Si photodiode was utilized to measure the pulse temporal behaviors, whose signal was connected to a digital oscilloscope (LeCroy) with the sampling interval of 0.1 ns and the bandwidth of 1 GHz.

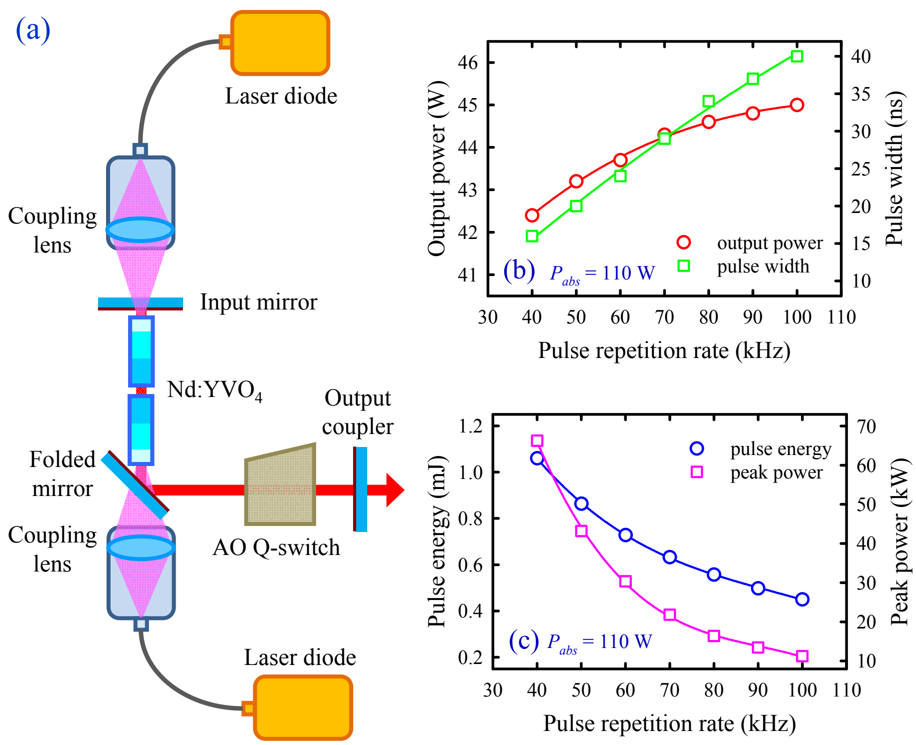

Fig. 4. (a) Schematic diagram for the dual-end-pumped actively Q-switched multi-segmented Nd:YVO_4 oscillator; Dependences of (b) the output power and pulse width, (c) pulse energy and peak power on the pulse repetition rate.

At first, the CW operation without the AO Q-switch is studied. The output power is experimentally found to be linearly proportional to the absorbed pump power without any signature of power saturation or roll-over phenomena. The maximum output power reaches 45.7 W under an absorbed pump power of 110 W, and the corresponding slope efficiency and the optical conversion efficiency are up to 59.4% and 41.5%, respectively. Figures 4(b) and

#190751 - $15.00 USD Received 17 May 2013; revised 16 Jun 2013; accepted 21 Jun 2013; published 27 Jun 2013

(c) illustrate the laser characteristics at an absorbed pump power of 110 W in the actively Q-switched operation. By increasing the pulse repetition rate from 40 to 100 kHz, the output power and pulse width are found to change from 42.4 to 45 W and from 16 to 40 ns, whereas the pulse energy and peak power are calculated to decrease from 1.06 to 0.45 mJ and from 66.3 to 11.3 kW, respectively. With a knife-edge method, the output beam quality for this high-power actively Q-switched laser was experimentally measured to be approximately 1.8, more effort should be made for improving the beam quality. Note that the polarization extinction ratios in either the CW or actively Q-switched operations were generally found to be larger than 200:1, and the emission polarizations were parallel to the *c* axis of the crystal. In the future, the multi-segmented crystals can be served as the amplified media in a chain of master-oscillator power-amplifiers to further scale the output power to the level of several hundred watts [10,11]. Such high-power infrared laser is also desirable to be applied in the process of extracavity harmonic generations to extend the emission lines into green and ultraviolet regimes [12–14].

5. Conclusion

In summary, we have successfully realized the concept of the multiple segments with different doping concentrations in the Nd:YVO_4 crystal for the first time. We have made a systematic comparison to manifest the large potential of the multi-segmented crystal for power scaling in end-pumped solid-state laser without bringing in considerable thermal effects. We further construct a high-power, high-repetition-rate dual-end-pumped AO Q-switched oscillator based on our novel YVO_4/0.1% + 0.3% Nd:YVO_4 crystal to efficiently generate the output power as high as 45 W and the pulse energy as large as 1.04 mJ, which confirms the usefulness of our crystal design.

Acknowledgments

The authors thank the National Science Council for their financial support of this research under Contract No. NSC-100-2628-M-009-001-MY3.